

Effect of the green porous texture on porcelain tile properties

J.L. Amorós*, M.J. Orts, J. García-Ten, A. Gozalbo, E. Sánchez

*Instituto de Tecnología Cerámica, Asociación de Investigación de las Industrias Cerámicas,
Universitat Jaume I, Castellón, Spain*

Received 8 March 2006; received in revised form 7 July 2006; accepted 15 July 2006
Available online 20 September 2006

Abstract

Porcelain tile is a product characterised by low water absorption (usually less than 0.1%) and excellent mechanical properties. To enhance tile aesthetic qualities, much of the porcelain tile production is polished to provide a high-gloss surface finish, in which certain closed pores in the tile body become visible. This apparent porosity of the polished tile, which had been closed porosity before polishing, sometimes lowers the product's stain resistance.

Test pieces were formed from a porcelain tile composition prepared under different milling conditions, pressing variables being kept constant, and the pore size distribution of these pieces was determined. The effect of the porous texture of the green pieces on the evolution of porosity during sintering and on the residual porosity of the densified body was analysed. It was verified that the porous texture of the fired piece was conditioned by the porosity and size of the largest pores in the green piece. The effect of residual porosity on stain resistance was determined by two cleaning methods. The presence of large pores in the green body, stemming from insufficient milling of the raw materials mixture, led to tiles with greater residual porosity and worse stain resistance.

© 2006 Elsevier Ltd. All rights reserved.

Keywords: Porosity; Pressing; Sintering; Microstructure-final; Tiles; Porcelain

1. Introduction

Porcelain tile is a product with excellent technical characteristics (zero or almost zero apparent porosity, high mechanical strength and frost resistance, high hardness, chemical and stain resistance, etc.) with a broad spectrum of aesthetic possibilities (body colouring with soluble stains, pressed relief, polishing, glazing, etc.).¹ These technical and aesthetic features have made porcelain tile a popular product, whose production grows annually. Porcelain tile formulation is based on three major raw materials that contribute the necessary plasticity for green processing and the required degree of meltability to provide the end product with its desired properties. The major raw materials are white-firing clays, and sodium and sodium–potassium feldspars. Other raw materials, used in minor quantities, are silica and feldspar sands, kaolins, and potassium feldspars.

Porcelain tile technical characteristics are closely related to the porous texture of the fired product. Thus, porcelain tile's

high mechanical strength is the result of low true porosity. Its frost resistance stems from zero or almost zero apparent porosity. Porcelain tile stain resistance is also a consequence of low porosity and the fact that the closed pores that surface when the tile is polished are small and isolated, making it difficult for dirt to enter the pores.^{2,3} However, the surface roughness of the polished piece affects stain resistance; thus, stain resistance increases when the number of cracks, chips and other irregularities produced during polishing decreases.^{4,5}

Fired porcelain tile porous texture is the result of the product's green microstructure and appropriate heat treatment. Fig. 1 schematically depicts the evolution of porcelain tile porosity during firing in terms of apparent porosity (interconnected pores) and closed porosity (occluded pores). Optimum firing temperature is the temperature at which no apparent porosity remains and closed porosity has not yet started to increase. The optimum firing temperature for porcelain tile usually lies between 1190 and 1220 °C. The product's porous texture at this temperature determines its technical properties.

Porcelain tile densification involves a liquid phase sintering process. During firing, at temperatures of about 900–1000 °C, an important quantity of liquid phase begins to form, surrounding

* Corresponding author.

E-mail address: jlamoros@itc.uji.es (J.L. Amorós).

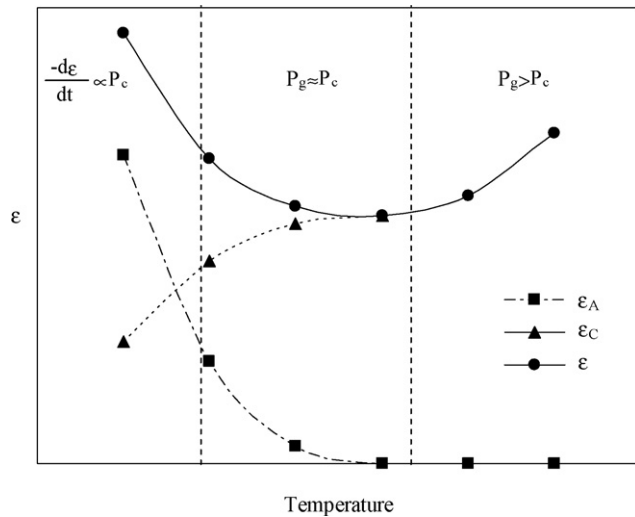


Fig. 1. Evolution of porcelain tile porosity during firing (general example). ε : true porosity; ε_A : apparent porosity; ε_C : sealed porosity.

the particles and producing a process-driving capillary pressure (P_c) at the contact points. The capillary pressure brings the particles closer together, increasing shrinkage and lowering porosity, while concurrently altering pore size and shape.⁶ Raising temperature increases the quantity of liquid phase and lowers porosity. In intermediate states, at around 1180 °C, pores start closing as inter-pore connections are eliminated. The occluded pores contain air that exerts a pressure (P_g) on the pore walls, opposing densification. In advanced process states, above 1200 °C, occluded pore gas pressure is high and counteracts capillary pressure, making the product expand. The sintering rate of this type of material⁷ is found from:

$$-\frac{d\varepsilon}{\varepsilon dt} = \frac{3}{4\eta_s}(P_c - P_g) \quad (1)$$

where ε is porosity, η_s system effective viscosity, P_g occluded pore gas pressure and P_c is capillary pressure, which is given by $P_c = -2\gamma/r$, where γ is surface tension and r is pore radius.

The study addresses the effect of green porcelain tile microstructure on the sintering process and on fired product properties.

2. Materials and procedure

A standard industrial porcelain tile composition has been used, consisting of 45 wt% white-firing clay, 40 wt% sodium feldspar and 15 wt% feldspathic sand. Four suspensions (R1–R4) were prepared by milling these compositions in a planetary ball mill for different times, in each case determining the residue on a 40 μm screen. Fig. 2 presents the corresponding particle size distributions, determined by laser diffraction. Raising the degree of milling is observed to reduce the coarse particle fraction, without altering the fine particles (clayey mineral). This yields narrower particle size distributions, producing more porous packings.

The suspensions were spray dried and disk-shaped test specimens were pressed from the resulting material. The following

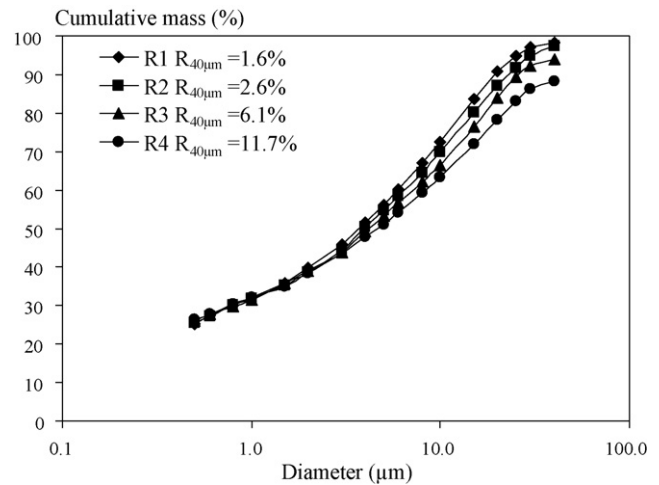


Fig. 2. Particle size distributions of the prepared mixtures ($R_{40\mu\text{m}}$: residue on 40 μm screen).

standard industrial porcelain tile pressing conditions were used: pressing powder moisture content of 0.055 kg water/kg dry solid and pressing pressure of 45 MPa. The test specimens were dried at 110 °C to constant weight. Specimen dimensions and bulk density were then determined by the mercury displacement method.⁸ The pieces were fired in an electric laboratory kiln at different peak temperatures, ranging from 1000 to 1260 °C. The heating rate was 25 °C/min, with a 6 min hold at peak temperature. Firing shrinkage (LS) and bulk density (ρ_c) of the pieces were determined by the mercury displacement method.⁸ Apparent porosity, measured as water absorption (WA) according to standard UNE-EN ISO 10545-3, was also determined.

Specimen porous texture was characterised by measuring bulk density, absolute density, water absorption, and determining pore size distribution (PSD) by mercury porosimetry in the pieces with a large apparent pore fraction, i.e. in the green specimens and in the specimens fired at peak temperatures up to 1175 °C.

Absolute density was determined in a Quantachrome Ultracycrometer 1000 helium pycnometer. True porosity was obtained from the bulk density and absolute density data. Mercury porosimetry was performed in a Micromeritics AutoPore III. Sample weight was about 2 g and a 130° contact angle was taken.^{9,10}

The PSDs were fitted to log-normal distributions.¹¹ The value of d_{16} was considered representative of the coarse pore fraction in the distribution, since previous studies⁶ had shown that the changes in porous texture during densification were better characterised by the evolution of this parameter than by that of total pore volume or by the average value of the distribution. The value corresponds to the diameter above which 16% of total pore volume is found. This parameter corresponds to the statistical value of the average plus the standard deviation of the normal distribution.

To determine the effect of fired specimen porous texture on stain resistance, the pieces were polished using diamond abrasive to size 3 μm . The polished surfaces were observed in an optical microscope with the bright field signal (BF).

The CIEL**a***b** chromatic coordinates were determined on the polished specimens with a diffuse reflectance spectrophotometer, using a CIE 10° standard observer and CIE type D65 standard illuminant. One millilitre rhodamine solution at 0.1 g/L (red dye that simulates wine stains) was deposited on the polished surfaces for a contact time of 30 min. The stained surfaces were then cleaned by two methods:

- (a) with a cloth dampened with water;
- (b) rubbing the specimen surface with a cloth impregnated with a cleaning agent, at a set pressure, with a constantly rotating mechanical device (180 rpm). The cleaning agent was a commercial bleach at a concentration of 35 g Cl₂/L. The application pressure was 0.8 kg/cm² (equivalent to strong manual pressure) and application time was 1 min.

*L***a***b** chromatic coordinates were measured again in the initially measured area, after applying the above cleaning methods.

Cleanability and stain retention were assessed as the difference in colour Δ*E**¹² of the polished specimen before staining and after cleaning from the following equation:

$$\Delta E^* = \sqrt{(L_0^* - L^*)^2 + (a_0^* - a^*)^2 + (b_0^* - b^*)^2} \quad (2)$$

where *L*₀**a*₀**b*₀* are specimen chromatic coordinates before staining and *L***a***b** are its chromatic coordinates after cleaning.

Dirt retention was evaluated as the Δ*E** of the specimen before applying rhodamine and after cleaning the surface with a cloth dampened with water.

Cleanability was assessed as Δ*E** of the specimen before applying rhodamine and after cleaning the stained surface by the (b) procedure. The larger the value of Δ*E**, the harder it is to clean the specimen.

3. Results

3.1. Green microstructure

Table 1 details the residue data of the mixtures on a 40 μm screen, together with the dry bulk densities of the pressed test specimens (ρ_s).

Fig. 3 plots the pore size distributions of the four prepared mixtures. The R3 and R4 curves are shifted towards the right, i.e. the specimens have larger pores than the longer milled mixtures (R1 and R2). R3 and R4 are observed to be less porous (smaller

Table 1
Residues on the 40 μm sieve of milled mixtures and dry bulk density (ρ_s) of the pressed specimens

Mixture	Milling time (min)	Residue on 40 μm (wt%)	ρ _s (kg/m ³)
R1	30	1.6 ± 0.2	1885 ± 4
R2	26	2.6 ± 0.2	1903 ± 5
R3	16	6.1 ± 0.3	1934 ± 3
R4	10	11.7 ± 0.5	1962 ± 2

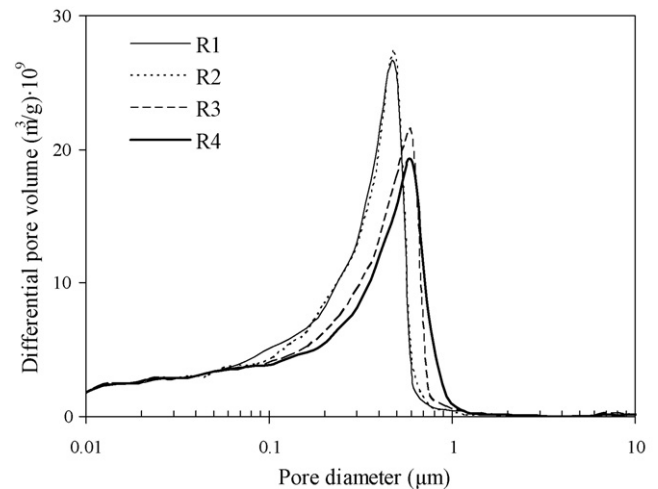


Fig. 3. Pore size distribution of the green specimens.

area under the curve). These results are consistent with the bulk density data obtained.

It can be inferred from the curves in Fig. 3 and the bulk density data (Table 1) that at the same pressing variables, the larger the composition coarse particle fraction (higher residue on 40 μm or shorter milling), the less porous (higher bulk density) are the resulting specimens, which, however, contain larger pores. In contrast, with longer milling (R1 and R2) the resulting specimens are more porous (lower dry bulk density), but the pores are smaller.

These outcomes are in agreement with the literature¹³ and confirm that particle size is directly related to pore size in the green packing.

3.2. Evolution of specimen microstructure with firing temperature

In order to analyse the evolution of porosity in the pieces with firing temperature, composition R1 was selected, which exhibited a residue on 40 μm similar to that of the compositions used in industry to make porcelain tile. Fig. 4 plots the pore size

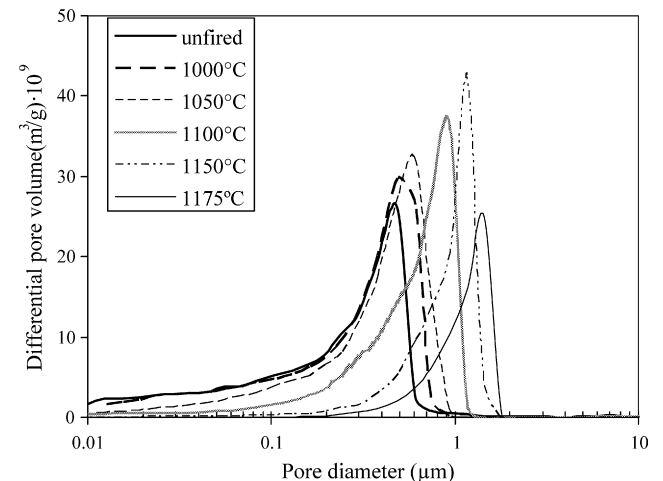


Fig. 4. Pore size distribution of the R1 series of specimens.

Table 2
R1 series

T (°C)	Green	1000	1050	1100	1150	1175	1200	1220	1240
ε	0.289 ± 0.005	0.302 ± 0.007	0.297 ± 0.007	0.281 ± 0.006	0.226 ± 0.009	0.153 ± 0.008	0.103 ± 0.007	0.100 ± 0.005	0.111 ± 0.006
ε_A	0.289 ± 0.005	0.280 ± 0.015	0.267 ± 0.015	0.249 ± 0.013	0.198 ± 0.014	0.147 ± 0.013	0.009 ± 0.012	0.000 ± 0.0010	0.000 ± 0.0010

True porosity (ε) and apparent porosity (ε_A).

distributions of the R1 series, comprising the green specimen and the specimens fired at different temperatures. Specimen apparent porosity (ε_A) and true porosity (ε) are given in Table 2.

Table 2 and Fig. 4 show that, for the R1 series, raising firing temperature reduces porosity, while the curves progressively shift towards larger pore sizes, i.e. pores grow owing to progressive elimination of the smallest pores. Porosity of the specimens fired at 1000 and 1050 °C is larger than that of the green specimen as a result of clay mineral decomposition, which increases porosity at 500–700 °C. The other compositions display a similar evolution.

Pore growth with temperature in incipient densification states, when liquid phase forms, has been observed in clayey compositions⁶ and glassy materials.^{14,15} In these materials with an initial broad pore size distribution, the formation of liquid phase eliminates the smaller pores, leading to particle rearrangement with the ensuing differential shrinkage of the material and growth of the larger pores.^{16–18} This coarsening is the result of heterogeneous pore sizes in the green packing.

As temperature rises a greater amount of liquid phase is produced and liquid-phase viscosity decreases. This enables eliminating larger pores, increasing shrinkage and lowering apparent and true porosity, while the remaining pores grow. The initially interconnected porous system progressively loses connectivity as sintering advances and pores start closing.

At 1200 °C apparent porosity is cancelled and the evolution of the porous texture needs to be monitored by examining polished

specimen cross-sections. Fig. 5 shows that raising temperature lowers specimen porosity further until maximum densification is reached, in this case at 1220 °C. A subsequent rise in temperature then lowers effective viscosity, making the specimen more deformable and raising occluded pore gas pressure above capillary pressure, so that the specimen expands. The optimum firing temperature for this type of product is maximum densification temperature (T_{max}). The starting composition formulation needs to make this temperature higher than the temperature that cancels apparent porosity, otherwise the fired product will have open pores, as is the case of group B1b floor tiles, defined in standard ISO 13006.

3.3. Effect of green microstructure on the evolution of porous texture during firing and on fired product properties

Fig. 6 plots the pore size distributions of the four series of test specimens fired at 1175 °C. Table 3 lists the bulk density data.

At intermediate sintering states, in which an important fraction of the initial porosity has been eliminated, the longest milled mixture (R1), which was the most porous green specimen, has densified most. This is essentially because the arising liquid phase sequentially eliminates pores by size. Hence, even when starting at higher porosity, if the pores are smaller, they will be eliminated at lower temperatures. Moreover, the apparent pores that remain at 1175 °C (Fig. 6) are smaller for mixture R1.

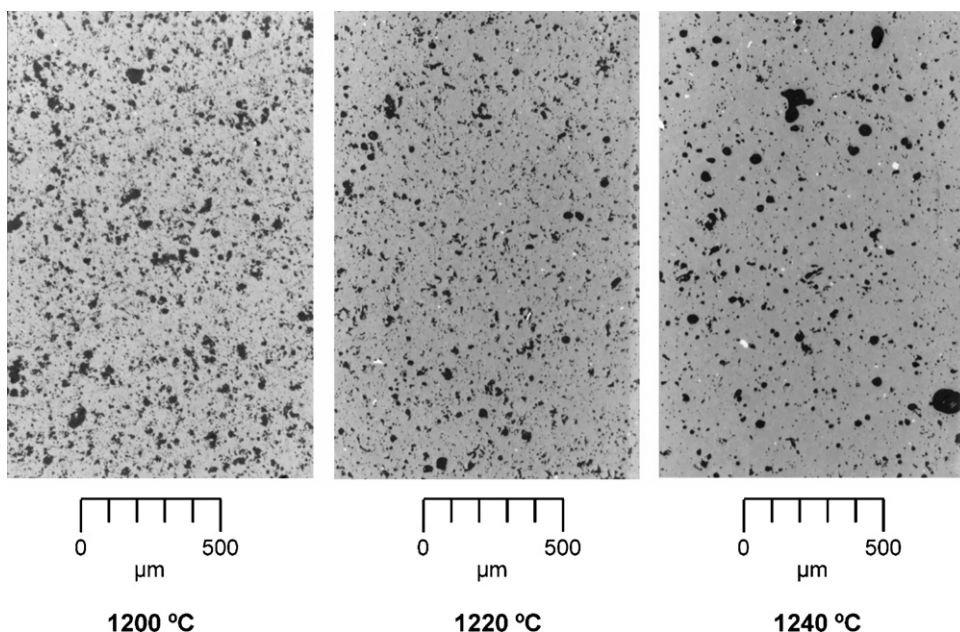


Fig. 5. BF images of polished cross-sections of R1 specimens.

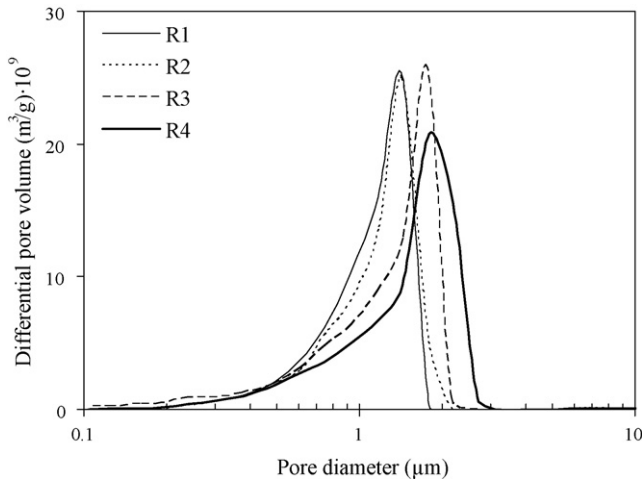


Fig. 6. Pore size distributions of the specimens fired at 1175 °C.

These findings explain why highly milled mixtures are used industrially to produce porcelain tiles. Thus, starting packings that contain small pores allow most of these pores to be eliminated during firing, yielding highly densified products.

To analyse the effect of green microstructure on pore growth during sintering, the values of d_{16} (statistical parameter selected as representative of the large pores) versus degree of densification, expressed as percentage eliminated porosity $(\epsilon_0 - \epsilon)/\epsilon_0$, where ϵ_0 is green porosity and ϵ is fired porosity, have been plotted in Fig. 7. Raising the degree of densification causes the coarsest pores to grow.¹⁹ The greater the initial particle packing heterogeneity, i.e. when the green body contains larger pores – the case of the less milled mixtures (R4) – the higher is the pore growth rate (curve slope).

The results obtained confirm that pore size growth during sintering depends on pore size in the green body, so that fired product porosity (Table 3) will depend more on pore size than on pore volume of the green body.

Fig. 8 plots bulk density and apparent porosity, expressed as water absorption, versus firing temperature for the four studied compositions. The plots correspond to the last stretch of intermediate- and final-stage sintering. The greater the degree of milling, the higher is the specimen’s maximum apparent density and the lower is the temperature at which this is attained (T_{max}). The vitrification temperature (T_v) or temperature at which apparent porosity is cancelled is also lower in this case.

Fig. 9 shows the appearance of the porous texture of the specimens fired at maximum densification temperature (T_{max}) and subsequently polished. It can be observed that as the residue on 40 µm increases (decreasing degree of milling) fired specimen pores become larger. These findings match the data presented in

Table 3
Bulk density of the specimens fired at 1175 °C

	Specimen			
	R1	R2	R3	R4
ρ_c (kg/m ³)	2305 ± 8	2282 ± 9	2235 ± 10	2206 ± 9

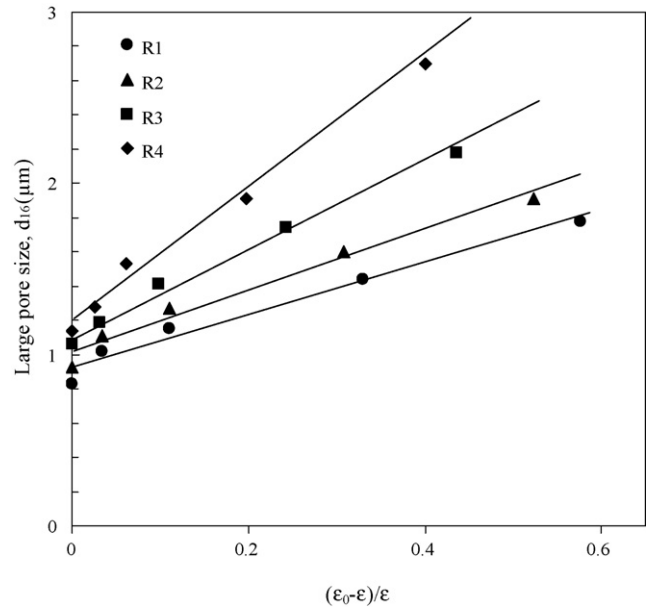


Fig. 7. Variation of statistical parameter d_{16} (representative of large pores) with degree of densification.

Figs. 4 and 7. Once again the results highlight the importance of the green porous texture on the characteristics of the fired product, particularly when this is polished. Polishing causes some of the initially closed pores in the product to surface. It is therefore important to have few pores and for these to be small to keep dirt from entering.

Fig. 10 plots maximum densification temperature (T_{max}) and vitrification temperature (T_v) versus degree of milling, expressed as residue on 40 µm, which is the parameter used industrially to control this process stage. As in Fig. 8, both T_{max} and T_v increase with the residue, i.e. they decrease when the degree of milling rises. T_{max} and T_v coincide for a residue of 4.2%. At higher degrees of milling (i.e. below 4.2%), vitrification temperature is lower than maximum densification temperature. This indicates that the fired product will have no apparent porosity and that the degree of milling will only affect the polished product as set out above. However, at lower degrees of milling (residue exceeding

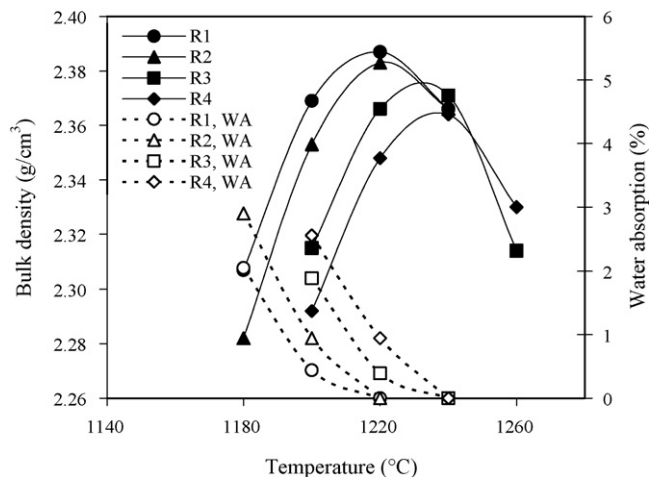


Fig. 8. Variation of bulk density and water absorption with firing temperature.

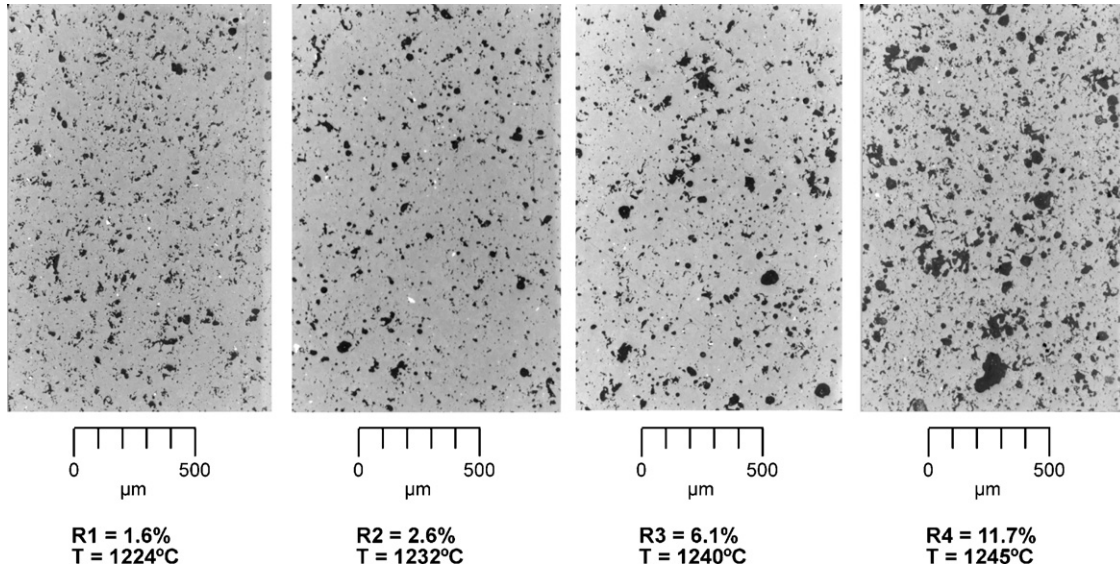


Fig. 9. Polished cross-sections (BF images) of specimens fired at T_{max} .

4.2%), T_{max} is lower than T_v so that products will exhibit apparent porosity at maximum densification even without polishing.

To analyse the relation between porous texture after polishing and stain resistance, Fig. 11 plots cleanliness and dirt retention of the specimens made with the longest milled mixture (R1). Dirt retention decreases when firing temperature is raised, and presents a minimum at T_{max} . This initial decrease is due to the reduction in specimen porosity, while the rise at $T > T_{max}$ is caused by specimen bloating, owing to occluded pore gas pressure, as indicated above.

With regard to cleanliness, ΔE^* decreases (cleanability increases) up to T_{max} and is held at higher temperatures in the studied range for this variable. ΔE^* does not decrease above T_{max} because when the body expands, porosity increases as a result of rising pore size and not because of greater pore number, while dirt can be more readily removed from large pores than from small ones.

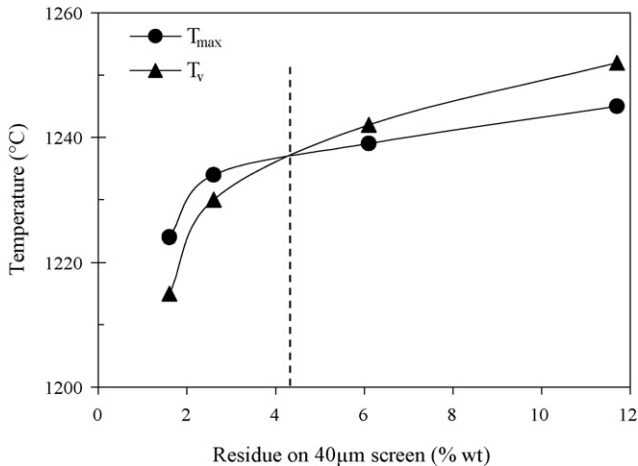


Fig. 10. Evolution of maximum densification (T_{max}) and vitrification temperature (T_v) with degree of milling.

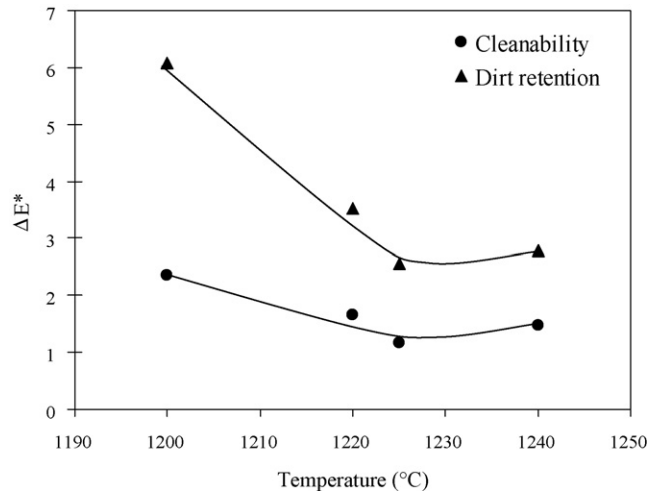


Fig. 11. R1 composition. Variation of dirt retention and cleanliness with firing temperature in polished specimens.

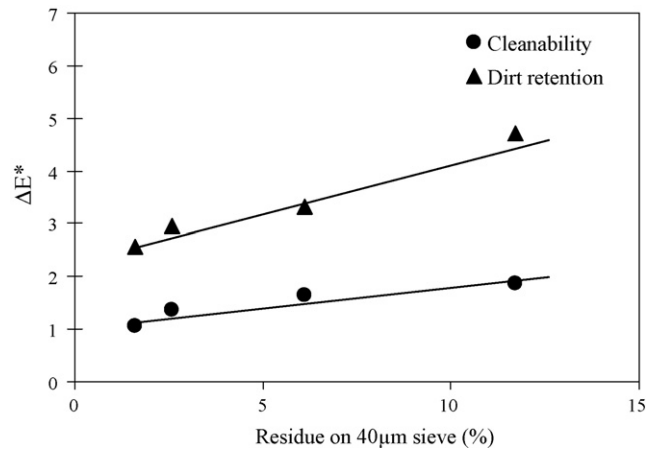


Fig. 12. Variation of dirt retention and cleanliness with degree of milling in specimens fired at T_{max} and polished.

To confirm the effect of green microstructure on the porous texture of polished specimens, Fig. 12 plots dirt retention and cleanability of the specimens prepared with the four mixtures and fired at T_{\max} versus degree of milling. Dirt retention increases and cleanability diminishes as degree of milling decreases (rising residue on 40 μm). The least milled mixtures are not only the most porous, but they also contain the largest pores, again confirming the enormous importance of green porous texture on end product properties, particularly when the product is to be polished.

4. Conclusions

The study shows that an insufficient degree of milling in porcelain tile compositions produces green bodies with a wide pore size distribution, containing large pores, even when the green bodies are more compact than ones made with longer milled compositions, under the same pressing conditions.

The presence of large pores in the green body hinders the sintering process, and requires a higher firing temperature to reach maximum product densification. Moreover, the minimum attainable porosity is higher and the size of the remaining pores increases. The negative effect of this porosity appears mainly as worse stain resistance of the polished product.

Fired porcelain tile porous structure is shown to be determined by the microstructure of the green body. The results explain why highly milled mixtures are used industrially to produce this type of product.

References

- Nassetti, G. and Palmonari, C., Decoration of porcelain stoneware tile. *Ceram. Acta*, 1997, **9**(5), 15–21.
- Beltrán, V., Ferrer, C., Bagán, V., Sánchez, E., García-Ten, J. and Mestre, S., Influence of pressing powder characteristics and firing temperature on the porous microstructure and stain resistance of porcelain tile. In *Proceedings of the IV World Congress on Ceramic Tile Quality. Cámara Oficial de Comercio y Navegación*, 1996, pp. 133–148.
- Esposito, L., Tucci, A., Rastelli, E., Palmonari, C. and Selli, S., Stain resistance of porcelain stoneware tile. *Am. Ceram. Soc. Bull.*, 2002, **81**(10), 38–42.
- Dondi, M., Ercolani, G., Guarni, G., Melandri, C., Raimondo, M., Rocha, E., Almendra, E. R. and Cavalcante, P. M. T., The role of surface microstructure on the resistance to stains of porcelain stoneware tiles. *J. Eur. Ceram. Soc.*, 2005, **25**(4), 357–365.
- Dondi, M., Guarini, G., Raimondo, M., Almendra, E. R. and Cavalcante, P. M. T., Stain resistance of porcelain stoneware tiles: the influence of microstructure. *Key Eng. Mater.*, 2004, **264–268**, 1511–1514.
- Orts, M. J., Escardino, A., Amorós, J. L. and Negre, F., Microstructural changes during the firing of stoneware floor tiles. *Appl. Clay Sci.*, 1993, **8**, 231–245.
- Orts, M. J., Amorós, J. L., Escardino, A., Gozalbo, A. and Feliu, C., Kinetic model for the isothermal sintering of low porosity floor tiles. *Appl. Clay Sci.*, 1993, **8**, 231–245.
- Albaro, J. L., Blasco Fuentes, A., Manfredini, T. and Pozzi, P., Una nuova metodologia sperimentale per la misura della densità apparente dei pezzi ceramici. Aspetti tecnici e applicativi. *Ceramurgia*, 1987, **17**(1), 4–8.
- Webb, P. A. and Orr, C., *Analytical Methods in Fine Particle Technology*. Micromeritics Instrument Corp., 1997.
- Gregg, S. J. and Sing, K. S. W., *Adsorption, Surface Area and Porosity (2nd ed.)*. Academic Press, London, 1982.
- Van Brakel, J., Modrý, S. and Svatá, M., Mercury porosimetry: state of the art. *Powder Technol.*, 1981, **29**, 1–12.
- Hunter, R. S. and Harold, R. W., *The Measurement of Appearance*. John Wiley & Sons, New York, 1987, pp. 162–194.
- Sánchez, E., García-Ten, J., Barba, A. and Beltrán, V., Estimation of packing density of raw material mixtures used in tile manufacture. *Br. Ceram. Trans.*, 1998, **97**(4), 149–154.
- Sacks, M. D. and Tseng, T. Y., Preparation of SiO_2 glass from model powder compacts. Part 2: Sintering. *J. Am. Ceram. Soc.*, 1984, **67**(8), 532–537.
- Sacks, M. D. and Tseng, T. Y., Preparation of SiO_2 glass from model powder compacts. Part 3: Enhanced densification by sol infiltration. *J. Am. Ceram. Soc.*, 1988, **71**(4), 245–249.
- Reijnen, P., Pore growth and elimination during sintering of silicate ceramics. *Cfi/Ber. DKG*, 1996, **73**(10), 594–598.
- Reijnen, P., Firatli, A. C., Goerg, H. and Arslan, R., The mechanisms of pore growth during vitrification. *Cfi/Ber. DKG*, 1984, **61**(8), 441–445.
- Whittemore, O. J., Porosity and pore size during ceramic processing. In *Advances in the Mechanics and the Flow of Granular Materials, vol. I*, ed. M. Shahinpoor. Trans Tech, Clausthal, 1983, pp. 249–258.
- Isik, G. and Messer, P. F., Effect of compaction pressure on the coarsening of open pores in fired compacts. *Proc. Brit. Ceram. Soc.*, 1978, **31**, 39–50.